ELSEVIER

Polymer 43 (2002) 2375–2383

polymer

www.elsevier.com/locate/polymer

Polymer melt rheology with high-pressure CO_2 using a novel magnetically levitated sphere rheometer

Joseph R. Royer[a], Yvon J. Gay[a], M. Adam[b], Joseph M. DeSimone[a,b], Saad A. Khan[a,*]

[a]*Department of Chemical Engineering, North Carolina State University, Raleigh, NC 27695-7905, USA*
[b]*Department of Chemistry, University of North Carolina, Chapel Hill, NC, 27599, USA*

Received 5 July 2001; received in revised form 29 November 2001; accepted 30 November 2001

Abstract

A magnetically levitated sphere rheometer (MLSR) designed to measure viscosity of fluids exposed to high-pressure carbon dioxide has been developed. This device consists of a magnetic sphere submerged inside a test fluid within a high-pressure housing and levitated at a fixed point. The housing is constructed from an optically transparent sapphire tube. The cylindrical tube can be moved vertically to generate a shear flow around the levitated sphere. The difference in magnetic force required to levitate the sphere at rest and under fluid motion can be directly related to fluid viscosity. Rheological properties, specifically zero shear viscosities, of transparent high-pressure materials can be measured to a precision of about 5% and over a wide range of viscosities. In addition, operation at constant pressure, in concentration regimes from a pure polymer to an equilibrated polymer/supercritical fluid solution, and at shear rates over several orders of magnitude is possible, eliminating many of the disadvantages associated with other high-pressure rheometers. Experiments performed at different temperatures with a poly(dimethylsiloxane) melt at atmospheric pressure are compared with data from a commercial Couette rheometer to demonstrate device sensitivity and viability. Measurements of a PDMS melt plasticized by high-pressure CO_2 are performed to illustrate the utility of the new rheometer under high-pressure conditions. Experimental data are obtained at 30 °C, for pressures up to 20.7 MPa and CO_2 concentrations reaching 30 wt%. Viscosity reductions of nearly two orders of magnitude compared with the pure polymer viscosity at atmospheric pressure are observed. Additionally, the effects of pressure on a polymer/CO_2 system are directly investigated taking advantage of the constant pressure operation mode of the MLSR. This allows us, for the first time in experiments of polymers with supercritical fluids, to decouple the effects of CO_2 concentration and pressure in a single device. © 2002 Published by Elsevier Science Ltd.

Keywords: Viscosity; CO_2; Supercritical fluid

1. Introduction

In recent years, the promotion and use of environmentally friendly solvents in a variety of traditional chemical and engineering processes has received increased attention. Liquid and supercritical CO_2 is one of the leading solvents promoted as an environmentally friendly or 'green' alternative to conventional organic solvents [1]. Unfortunately, implementation of supercritical fluids (SCFs) in industrial processes has been problematic. These problems often result from large knowledge gaps in the physical properties and processing characteristics of SCF/polymer systems. Most importantly the effect of CO_2 and other SCFs on the rheological behavior of polymer melts and solutions have only been studied at very low or high concentrations of SCFs. In particular, minimal experimental data is available on viscosities of CO_2 solutions, which is required for equipment design, industrial scale-up, and process modeling of new SCF applications. A number of experimental devices capable of measuring rheological properties of complex fluids under high-pressure have been developed over the last 40 years to address this lack of knowledge [2–14]. Most of these devices can be classified into three categories: (a) pressure driven, (b) falling body, and (c) rotational devices. Each of these devices has specific advantages, which make them important techniques for rheological measurement. However, each also has significant disadvantages, which limits their usefulness, especially for CO_2/polymer solutions.

Pressure driven devices such as back-pressure regulated capillary rheometers [2,3,15–17] and extrusion slit dies [4–8] can measure polymer melts plasticized by CO_2 and other SCFs. These devices mimic conventional polymer processing giving much needed viscosity information for many polymer melts. However, the nature of a pressure driven flow limits their utility. In particular, the often large pressure drop limits the concentration of the dissolved SCF that can

* Corresponding author. Tel.: +1-919-515-4519; fax: +1-919-515-3465.
E-mail address: khan@eos.ncsu.edu (S.A. Khan).

0032-3861/02/$ - see front matter © 2002 Published by Elsevier Science Ltd.
PII: S0032-3861(01)00804-7

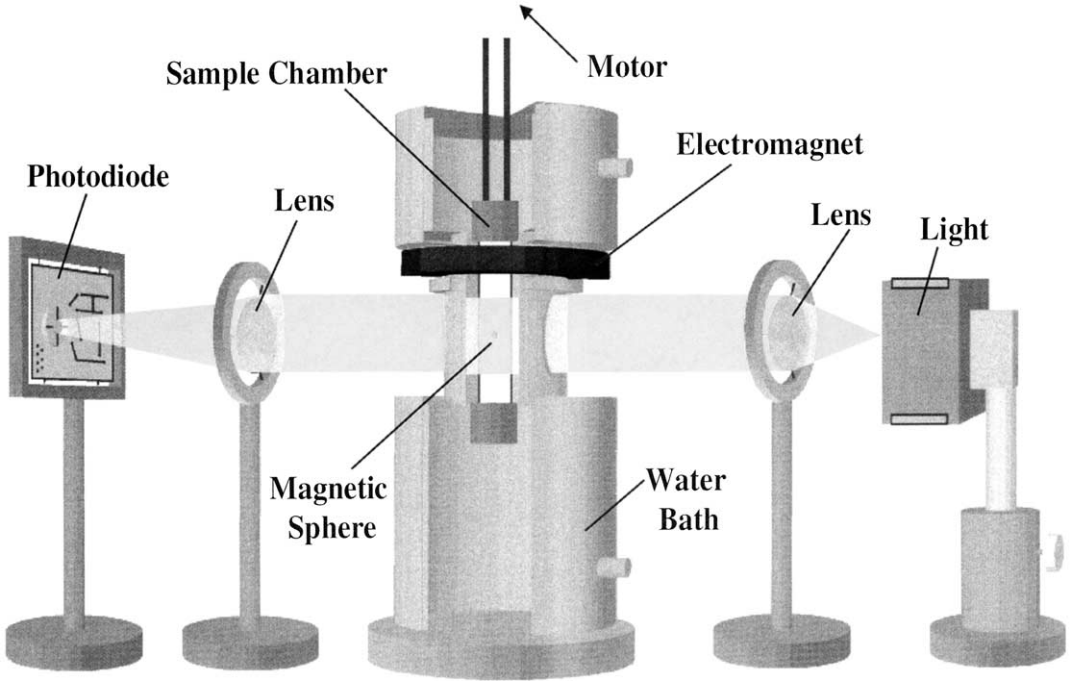

Fig. 1. Schematic diagram of the magnetically levitated sphere rheometer (MLSR) system, including optical detection system.

be measured. Therefore, the SCF concentration must be maintained at low values, far from equilibrium, to avoid phase separation during measurement. In this low SCF concentration region, these devices have been found to provide accurate and useful rheological information.

Falling body devices such as falling cylinder [9–11] or rolling sphere [18] devices are useful in measuring highly concentrated SCF solutions of low viscosity. They operate at constant pressure allowing direct measurement of pressure effects on rheology [11]. Unfortunately, the sinker density and fluid viscosity determine the shear rate, making the measurement of viscosity as a function of shear rate difficult [11]. Falling body devices are also limited to low-viscosity solutions because the fall times required to measure high viscosity systems are too long to be experimentally viable. Additionally, limited shear rate control makes data comparison between different experimental samples difficult.

Finally, rotational devices such as high-pressure couette [14] or parallel plate geometries [12,13] can operate at constant pressure and a variety of different shear rates. Unfortunately, rotational devices are difficult to design because viscoelastic or rotational information must be transferred under pressure. Mechanical information is often lost via transfer of torque through a dynamic seal, limiting measurement sensitivity. Additionally, a magnetically coupled drive shaft, which generates slightly non-uniform flow, is often used for motion control. These devices also generally require operation to occur at or near equilibrium conditions because a headspace of the pressurizing SCF must be maintained. The polymeric sample can often leak out of the measurement device and penetrate the SCF headspace due to polymer swelling, creating measurement errors.

Our study focuses on the development of a new class of rheometer for measuring the properties of SCF/polymer solutions and melts, the magnetically levitated sphere rheometer (MLSR). This device is based on the original designs of an ambient pressure MLSR proposed by Adam and Delsanti [19] and later modified by others, [20–22] used to measure the rheological properties of polymer gels and volatile polymer solutions [19,23–27]. The principles and device designs are also similar to low pressure magnetic float densimeters [28–32]. The high-pressure MLSR (shown schematically in Fig. 1) employs the basic cell design of a falling sphere rheometer, allowing the device to operate at constant pressure conditions and eliminating the headspace associated with the high-pressure rotational devices. In contrast to the falling body devices, however, the sphere is held stationary at a fixed point through magnetic levitation while the cylindrical sample chamber is moved vertically using a stepper motor to generate shear flow around the stationary sphere. The sample chamber velocity is coupled to the shear rate and the change in magnetic force necessary to maintain the sphere stationary is related to the shear stress, thus allowing measurement of steady shear viscosity. However, the device needs to be calibrated against a known fluid viscosity because of the non-homogeneous nature of the flow.

The device is not limited to low-viscosity materials, as in the falling body devices, because measurement time is only proportional to the response of the instrument's electronic control and not the viscosity of the system. The MLSR uses the magnetic force to detect the shear stress imposed on the

sphere by the sample chamber motion, eliminating the error of magnetically coupled motion associated with many high-pressure rotational devices. These advantages make the MLSR an excellent candidate for high-pressure rheometry because both the application of shear and the measurement of shear stress can be accomplished without transferring information directly across a mechanical seal.

In this paper, we discuss design aspects of the novel high-pressure magnetically levitated sphere rheometer (MLSR). The fabrication of both the MLSR and the high-pressure sample cell are examined in detail, together with calibration of the device. A comparison of data obtained using the MLSR and a commercially available rheometer at atmospheric pressure is shown to establish the accuracy of the new experimental device. Finally, we present results of a set of high-pressure experiments to demonstrate the utility of this device under pressurized conditions, for the measurement of zero shear viscosity of Newtonian fluids and use this data to examine some of the assumptions of previous experimental work with relation to pressure and CO_2 concentration.

2. Theory of magnetic levitation

2.1. Sphere levitation

To describe the operation of the MLSR [19], only simple force balances about the magnetically levitated sphere are required. For simplicity, a magnetic sphere of radius a is considered to be maintained at the origin of a three-dimensional coordinate system. Levitation of the sphere is accomplished by balancing the effective gravitational force on the sphere by an applied magnetic force from an exterior coil, as described by Eq. (1):

$$F_{M_o} = F_g - F_b \tag{1}$$

where F_{M_o} is the magnetic force required to levitate the sphere in a stationary fluid and F_g and F_b are the forces of gravity and buoyancy, respectively.

The magnetic sphere is held within a pressurized sample cell capable of vertical motion, as shown in Fig. 2. Imposed vertical motion of the sample cell (sapphire tube) induces a flow field within the test fluid, creating an additional force on the sphere. To maintain the sphere fixed at the origin, the total magnetic force, F_{M_T}, is adjusted to account for the viscoelastic force, F_v, imposed by the fluid, as revealed by the following relationship:

$$F_{M_T} = F_g - F_b + F_v \tag{2}$$

The change in the magnetic force, $\Delta F_M = F_{M_T} - F_{M_o}$, must exactly equal F_v. Therefore, the change in magnetic force created by the imposed shear force on the sphere can be used as a measurement of the rheological properties of the surrounding fluid.

The gradient of a magnetic field, H, along the axis, z, of a magnetic coil is given by:

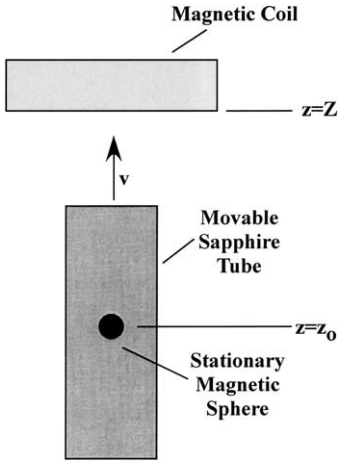

Fig. 2. Diagram showing the spatial relationship between the magnetic coil, the stationary levitated magnetic sphere, and the sapphire sample chamber capable of vertical motion.

$$\left(\frac{\partial H}{\partial z}\right) = Cn_o I \tag{3}$$

where C is a constant determined by the geometry of the coil and the position of the sphere along the axis, n_o is the number of windings in the coil, and I is the current supplied to the magnetic coil. This expression for the magnetic field gradient results in the following relationship for the total magnetic force on the sphere:

$$F_{M_T} = \frac{4\pi}{3} a^3 J \left(\frac{\partial H}{\partial z}\right)_{z=z_o} = AI \tag{4}$$

where J is the permanent magnetic dipole of the sphere and A is the proportionality constant between the magnetic force and the current supplied to the coil. The proportionality constant between the magnetic force and the current of the electromagnetic coil, A, is variable based on the position of the magnetic sphere in the magnetic field gradient. For consistency between experiments, the position z_o is defined, as shown in Fig. 2, at the same point during calibration and all experiments. Thus during the operation of the device, the magnetic sphere is always levitated at the same position from the magnetic coil. All other variables in Eq. (4), with the exception of the current supplied to the electromagnetic coil, I, are physical constants of the system that remain unchanged with the application of a viscous force. Thus, F_v can be described by the following expression:

$$F_v = \Delta F_M = A(I - I_o) \tag{5}$$

Here, I is the current supplied to the magnetic coil while a viscous force is present, and I_o is the current supplied to the magnetic coil when the fluid is at rest. Eq. (5) constitutes the general working equation for the MLSR; however, the expression for F_v depends upon the type of fluid being measured and the geometry of the magnetic coil and sphere.

2.2. Viscoelastic forces

To determine an expression for F_v, the type of fluid and rheometer geometry must be considered. In general, the viscoelastic force imposed on the sphere is proportional to the shear stress, σ, on the surface of the sphere as follows [19,33]:

$$F_v \propto a^2\sigma \tag{6}$$

The shear stress of a simple viscoelastic fluid for which the assumptions of strain additivity are valid can be written as [33]:

$$\sigma = \int_{-\infty}^{t} G(t-s)\dot{\gamma}(s)\mathrm{d}s \tag{7}$$

where $G(t)$ is the relaxation modulus and $\dot{\gamma}(t)$ is the shear rate.

2.2.1. Newtonian fluids

For a Newtonian fluid Eq. (7) reduces to the definition of viscosity $\eta = \sigma/\dot{\gamma}$ [33]. Substituting this relationship into Eq. (6) forms a governing relationship for the viscous force acting on the sphere:

$$F_v = \phi\eta r^2\dot{\gamma} \tag{8}$$

ϕ is a constant dependent upon the geometry of the rheometer. The maximum shear rate at the surface of the sphere, for a fluid with a maximum velocity at the tube wall of v, can be estimated as $\dot{\gamma} = 3v/2r$ [34]. Substitution of this relationship into Eq. (8) and combining with Eq. (5) yields the following working equation for a Newtonian fluid:

$$\eta = \frac{K(I - I_o)}{v} \tag{9}$$

K is a calibration constant, which is specific to the rheometer and sphere geometry and the magnetic properties of the coil and sphere, determined from measurement with fluids of known viscosity. Because the shear rate on the surface of the sphere is non-uniform, the exact measurement of the shear rate is difficult [35,36]. However, the governing equation uses the calibration of fluids of know viscosity to determine the calibration constant K, making the determination of a zero shear viscosity for a Newtonian fluid extremely accurate.

3. Rheometer design and construction

A schematic diagram of the MLSR is shown in Fig. 1. The main housing or temperature bath, based on the original designs of Adam and Delsanti [19], were machined in-house using non-magnetic stainless steel. The main housing is used for temperature control of the rheometer. Using ports on both the top and bottom of the main housing, cooling water, filtered for particles that would create noise in the optical detection system, is circulated around the sample chamber. The control of the sample chamber temperature can be maintained to ± 0.5 °C using this method. Machining of the magnetic spheres from solid pieces of samarium cobalt is accomplished by employing compressed air to move the samarium cobalt inside a simple sandpaper cylinder until the desired shape is obtained. Spheres machined in this manner have been made with diameters between 1.0 and 0.65 mm. The sphere used in the experimental work described here had a diameter of 0.78 mm. Examination of the sphere under a microscope (magnification 30×) revealed it to be spherical and free of large-scale surface defects. The time required to machine each sphere is approximately 24 h.

The xenon light source (Hamamatsu Corporation, L2174), which generates a uniform light intensity over extended periods of time, (~1000 h) illuminates the sphere. Light generated by the xenon bulb first passes through an achromatic lens (Edmund Scientific, K32-323) to collimate the light beam, and then a double-convex lens (Edmund Scientific, K32-625) magnifies the sphere's image onto the photodiode. A silicon quadrant photodiode (CentroVision, QD-50-0-SD) with built-in transimpedance amplifiers and an active area of 7.98 mm^2 detects the position of the sphere within the test fluid. A ± 15 V DC signal generated by a laboratory power supply (Oriel Instruments, 70703) provides stable power for the photodiode.

The electromagnetic coil was wound in-house using 20 gauge (0.75 mm diameter) copper wire with a PTFE coating and contains 150 windings. A Kepco, Inc. (Model BOP 20-5M) power supply, set in constant-current mode, generates a variable electrical current for the magnet. Vertical movement of the sample cell inside the main temperature housing is accomplished by a Physik Instrument (Model N-405.DG) linear translational stage. The linear translational stage can move with a minimum increment of 0.1 μm and a maximum velocity of 1.5 mm/s. Both data acquisition and control systems employ National Instruments (Austin, TX) BridgeView industrial automation software in conjunction with National Instruments Field Point modules. This integrated system sends a set of control signals to the motor and magnet (via the constant-current power supply) and receives information from the photodiode. The time resolution on both measurement and control of the sphere levitation is approximately 0.04 s. A TMC (Model #63-561) isolation table supports the entire device to dampen vibrations caused by surrounding laboratory instruments, and a plywood box lined with heavy fabric limits electronic noise caused by extraneous light.

3.1. High-pressure sample chamber

The modification of the magnetically levitated sphere rheometer to operate under high-pressure conditions requires the design of a novel sample chamber. The high-pressure sample chamber design centers on a sapphire tube, rated to a burst pressure of 42 MPa, which constrains the test fluid while maintaining high-pressure. The sapphire tube

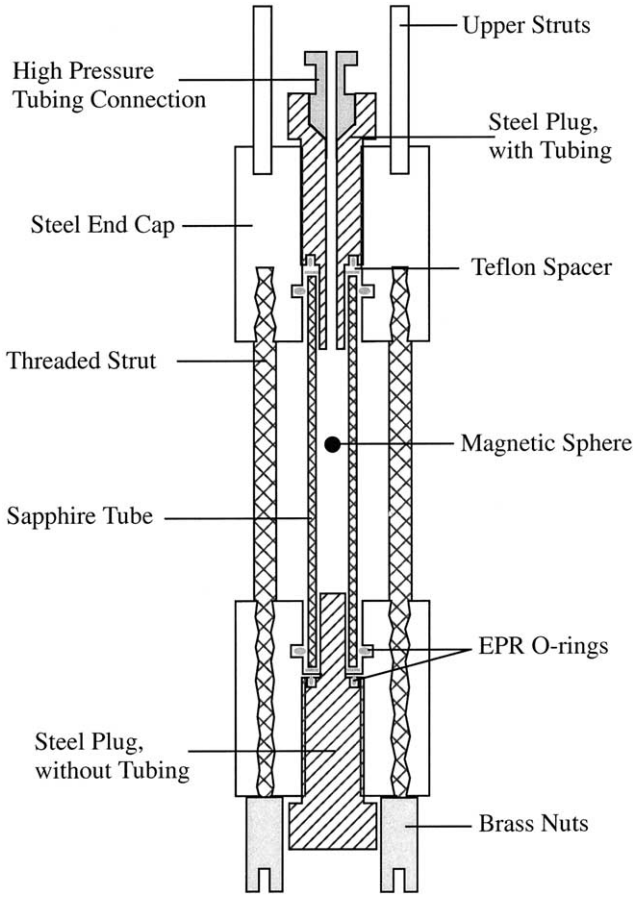

Fig. 3. Schematic diagram of the high-pressure sample chamber for the MLSR.

transmits light with good optical clarity for photodiode detection of the sphere's shadow. The volume of the sample chamber is approximately 1 mL. This small sample size is important for enhancing the rate of equilibration of the SCF solution because only minimal mixing inside the cell is possible.

The sample chamber design is similar to the high-pressure view cells used by Davis [37] and others [21, 38–41]. A schematic diagram of the high-pressure sample chamber is shown in Fig. 3. The sapphire tube ($L = 50$ mm, O.D. $= 6.3$ mm, I.D. $= 4.3$ mm) is clamped between two end caps, which are machined of non-magnetic stainless steel. Four threaded metal struts clamp the two end caps together and tighten the sapphire tube in place with four brass nuts. A PTFE spacer, inserted between the end caps and the tube, absorbs some of the force placed on the flat ends of the sapphire tube. Ethylene-propylene rubber, (EPR), O-rings on the inside of the end caps make a seal with the outer radius of the sapphire tube. Stainless steel plugs inserted into the end caps on both sides allow access to the tube and sample chamber once the sapphire is tightened in place. A second EPR O-ring is used to make a seal between the steel plugs and the end caps. The upper steel plug contains an opening for high-pressure tubing (1/16") that allows the cell to be filled with a pressurized fluid. The lower steel plug also contains an opening for tubing, making flow through of the chamber and real time sampling. The upper end cap has two additional struts connecting the cell to the linear translational motor.

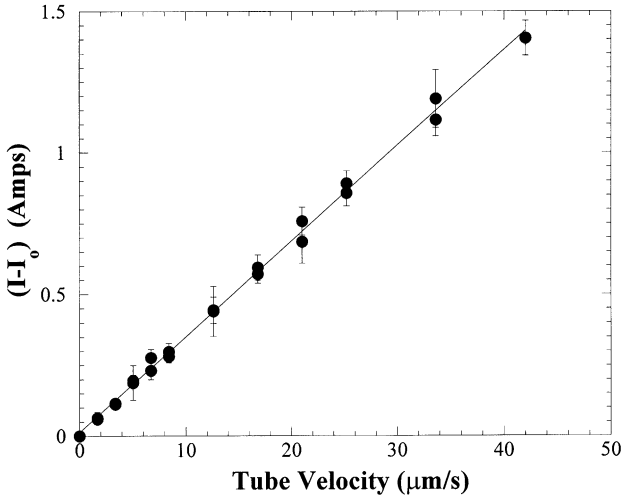

Fig. 4. A representative set of experimental calibration data shown for a 30 Pa s polydimethyl siloxane viscosity standard sample at 25 °C and atmospheric pressure. The difference between current supplied to the magnetic coil that required to levitate the sphere at rest (I_o) and under shear (I) is plotted against tube velocity (v). The linear slope confirms the sample to be Newtonian, and the plot represents a single calibration point for the determination of the geometric constant K.

4. Rheometer calibration and experimental verification

Because the ultimate reason for constructing this device is to measure viscosities of polymer melts with dissolved liquid and supercritical CO_2, a set of viscosity standards with a range of viscosities in the area of interest were chosen to calibrate the instrument. While the calibration is expected to be linear over a large range of viscosities the measurement of low viscosity material requires enhanced measurement sensitivity. This can be accomplished by an appropriate choice of magnetic material for the sphere in conjunction with an optimized electromagnet and subsequent recalibration. Five silicone oil viscosity standards obtained from Brookfield Engineering Laboratories (Middleboro, MA) corresponding to viscosities of 100, 60, 30, 12.5, and 5 Pa s were used as received.

Fig. 4 displays the experimental data obtained for a single experimental fluid (300 P standard) over a range of shear rates. A linear relationship between tube velocity (v) and the change in current supplied to the magnetic coil (ΔI) is observed, confirming the calibration fluid to be Newtonian. It is important to note that the magnitude of ΔI is of the same order of magnitude as the electronic noise in the measurement, generating a larger uncertainty and experimental scatter at the lowest shear rates. As the tube velocity is

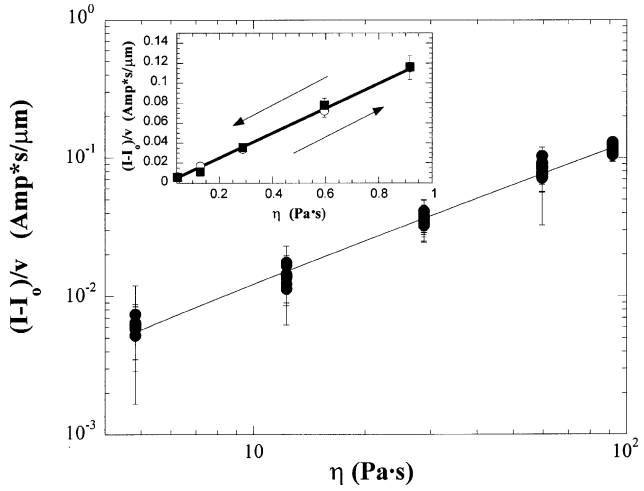

Fig. 5. Calibration curve for five silicone viscosity standards determined at 25 °C and atmospheric pressure plotted in terms of $(I - I_o)/v$ vs. viscosity. The inset displays lack of a hysteresis effect as the measurements are taken in both positive and negative flow directions.

increased, both the levels of uncertainty and the experimentally observed scatter are reduced. Therefore in all cases, experimental measurements were conducted at tube velocities, which generated ΔI at least two orders of magnitude larger than the scatter in the sphere positioning measurement.

Fig. 5 displays the entire calibration curve for all five viscosity standards. The linear fit to the experimental data results in a calibration constant, K (from Eq. (9)), of 7.75×10^2 (μm Pa/A). Over the entire set of viscosity standards, the deviation from the experimental calibration is approximately ±2.5%. The inset in Fig. 5 displays the absence of any hysteresis with tube motion. To accomplish both the calibration and the additional hysteresis detection experiment, the sample cell is first moved upward at a known velocity corresponding to the positive flow direction.

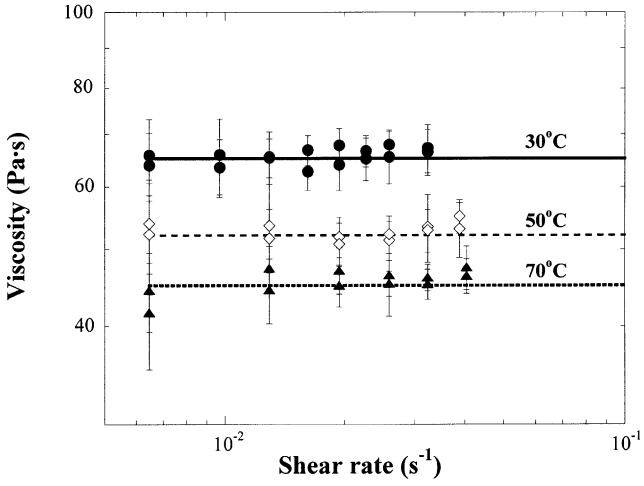

Fig. 6. Viscosity versus shear rate data of a PDMS sample obtained using a commercially available couette rheometer (lines) and the high-pressure MLSR (symbols) over a range of temperatures.

The current supplied to the magnetic coil is recorded for a 30 s period once the electronic signal becomes stable, typically within 5 s. The sample chamber is then immediately moved in the downward or negative flow direction at the same speed and a new supply current for the magnetic coil is measured. This procedure is then repeated for the other calibration standards. The calibration constant is independent of the tube direction, suggesting that errors in flow direction are not present during the experimental operation of the device. In addition, the sphere is always levitated a minimum distance of at least 10 times the diameter of the sphere, away from the ends of the sample chamber to minimize end effects that would occur near the edge of the sealed tube.

In order to demonstrate that the rheometer accurately measures the viscosity of a polymer melt, a test fluid was measured using both the MLSR and a commercially available rheometer equipped with a couette geometry (Rheometerics, DSR). VISCASIL-100M™, a silicone oil obtained from General Electric (Waterford, NY), was selected as the test fluid. VISCASIL-100M has a M_w of 160 kg/mol and a polydispersity of 2.3. Fig. 6 shows a set of viscosity points (solid symbols) measured using the MLSR at three different temperatures and atmospheric pressure, while the solid lines represent the Newtonian viscosity obtained using a traditional couette rheometer. Comparison of the two different measurements reveal a maximum error of 5% between the MLSR and the couette, with an error less than 2%, in most of the cases. This suggests that the calibrated MLSR measures the viscosity of the polymer test sample to an accuracy of approximately 2% over this range of temperatures. This level of experimental error is similar to that of previous devices [20,22,23]; however, the use of a sapphire tube does contribute some additional errors to the system. Rings or ridges present in the sapphire, which are generated from the growth method used to create the tube, imparts some optical noise to the detection system not present with glass tubes used in low pressure analogs.

5. Viscosity measurements

To demonstrate the high-pressure capability of the MLSR, the rheological effects of CO_2 incorporation into a polymer were measured. A known mass of the sample PDMS (Viscal-100M) was loaded into the sample cell. A vacuum was then pulled on the sample to remove any air dissolved in the system followed by subsequent pressurization with CO_2. Using a syringe pump (Isco, 260D), the amount of CO_2 required to pressurize the sample to the desired pressure was accurately measured. The loaded sample was allowed to equilibrate for 48 h; this equilibration time is sufficient to produce a homogeneous mixture free of CO_2 bubbles as measured by previous swelling experiments [42]. Occasional stirring was accomplished by agitation of the magnetic sphere within the sample cell.

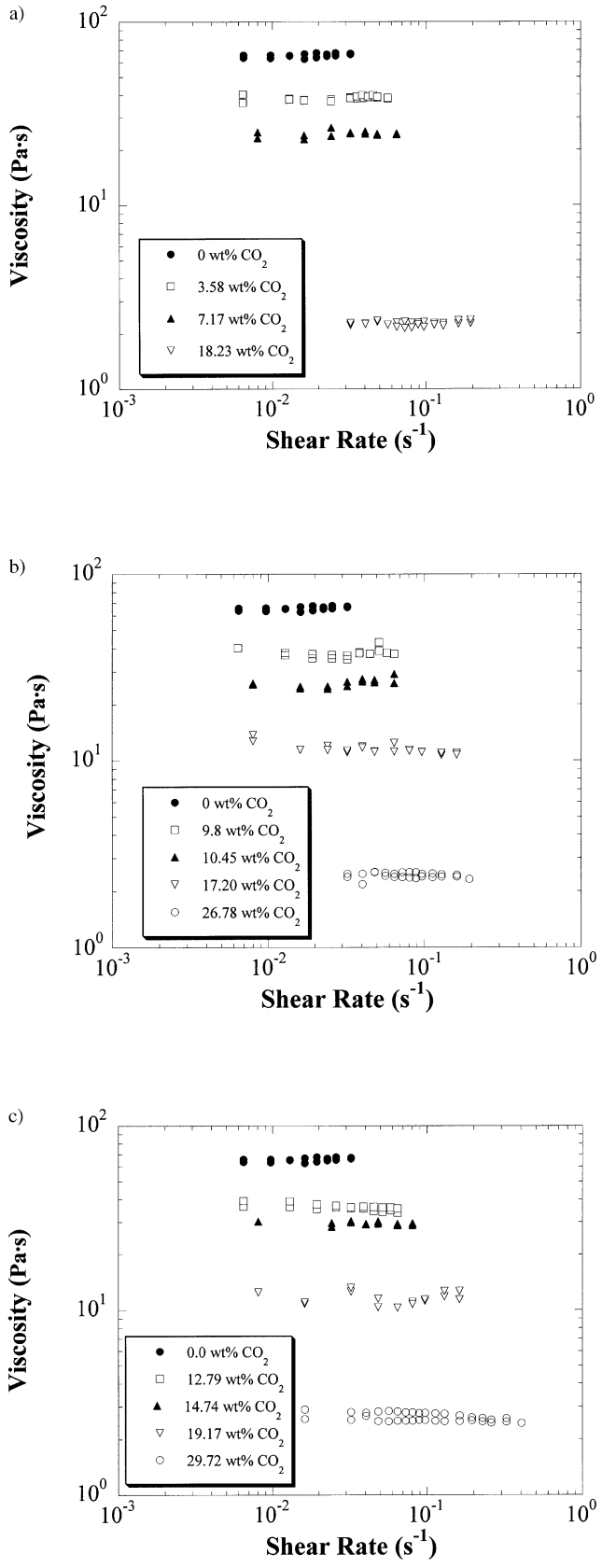

Fig. 7. Viscosity-shear rate behavior of a PDMS sample pressurized to different extents with CO_2. Experiments were conducted at 30°C. (a) 6.9 MPa, (b) 13.8 MPa, (c) 20.7 MPa.

The viscosity was measured at different positions in the fluid and found to be reproducible, thereby assuring the homogeneity of the sample.

Fig. 7a–c displays the experimentally obtained viscosity measurements of the PDMS sample at 30 °C over a range of CO_2 concentrations and pressures of 6.9, 13.8 and 20.7 MPa, respectively. Examination of the figures reveals the experimentally observed viscosity reduction of PDMS with the incorporation of CO_2 to be significant. For the measurements taken at 6.9 MPa, the viscosity reduction of the PDMS melt from data taken at 30 °C and atmospheric pressure is nearly 97% at a CO_2 concentration of 18.2 wt%. Unfortunately, the viscoelastic scaling models developed in previous experimental work are not applicable in this case [4], because the T_g depression model used is not valid for concentrations greater than 10–15 wt% CO_2 [43].

Previous studies with PDMS have effectively used a pressurized capillary rheometer to measure melt viscosity with CO_2 at 50 and 80 °C over a range of pressures and CO_2 concentrations [2,44]. The results reveal a substantial reduction in melt viscosity in the presence of CO_2. However, no attempt has been made to examine the effect of pressure on viscosity. When using a pressurized capillary device [2,3,44] or an extrusion slit die [4,6,8], which we have used previously, the nature of the flow creates a pressure gradient during measurement, making a determination of the pressure effect difficult. The actual pressure in the melt during measurement with these devices changes along the length of the die, requiring an average pressure to be used for investigations of pressure related effects. The MLSR on the other hand, with its constant pressure operational mode, allows direct examination of the effects of pressure on melt viscosity. This is illustrated in Fig. 8 in which we have plotted average viscosity versus CO_2 concentration for different pressures. It is clear from Fig. 8 that the effect of pressure on CO_2/PDMS is non-negligible. For instance, a viscosity of 40 Pa s at a pressure of 6.9 MPa is attained at a CO_2 concentration of approximately 4 wt% but would only be attained with 14 wt% CO_2 at 20.7 MPa.

Decoupling of the effects of CO_2 concentration and pressure is possible using the MLSR because both concentration and pressure can be varied independently, and thus can be clearly determined without the use of any theoretical modeling [38]. This is illustrated in Fig. 9 in terms of the pressure and concentration shift factors. Using Fig. 8, we can obtain a pressure shift factor a_p that collapses all of the experimental data to a single curve with respect to CO_2 concentration and the temperature of measurement. This is accomplished by fitting the experimental data at each pressure to an exponential function and then mechanically collapsing the data to a single pressure. The shift factors required to perform this viscoelastic scaling are then plotted and extrapolated back to atmospheric (zero) pressure. The pressure shift factors (a_p) are then normalized to ensure that a value of 1.0 is obtained at atmospheric pressure. Fig. 9a displays the pressure shift factor as a function of applied pressure, with

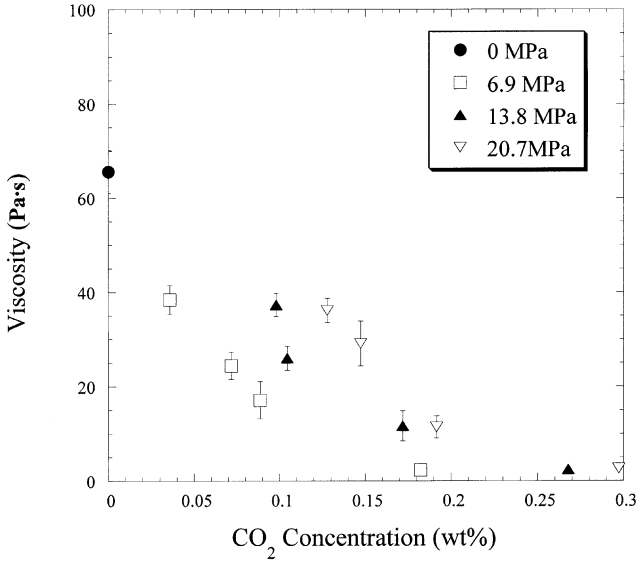

Fig. 8. Zero-shear viscosity of a PDMS sample as a function of CO_2 concentration at various CO_2 pressures.

the exact values of a_p given in Table 1. Performing the appropriate pressure shift with the calculated values of a_p results in a master curve as a function of CO_2 concentration at 30 °C. The concentration shift factor, a_c, can thus be determined by directly scaling the value of viscosity (shifted to atmospheric pressure) with the measured viscosity of PDMS at 30 °C, atmospheric pressure and in the absence of CO_2. Fig. 9b reveals how the concentration shift factor varies as a function of CO_2 concentration imbibed within the polymer, with the exact values of a_c given in Table 2.

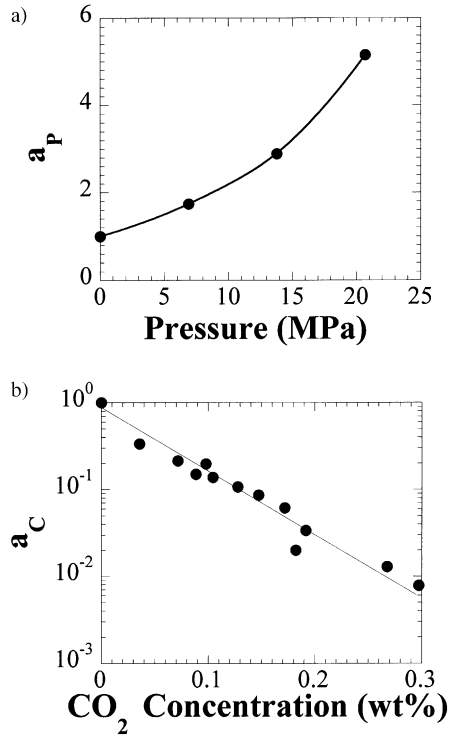

Fig. 9. Viscoelastic scaling parameters for a PDMS/CO_2 system at 30°C. (a) Pressure shift factor, a_p, (b) concentration shift factor a_c.

Table 1
Pressure shift factors for viscoelastic scaling of PDMS/CO_2 system at 30 °C

Pressure (MPa)	a_p
Atmospheric	1
6.9	1.74
13.8	2.89
20.7	5.15

The decoupling of pressure from concentration is important as it provides information on how each of these parameters independently affects polymer viscosity. For example, Fig. 9a reveals by what factor the viscosity would increase if we were to pressurize the PDMS sample with CO_2, but without any CO_2 getting imbibed into the melt, i.e. provides information on the hydrostatic pressure head effect. Thus, we observe that the PDMS viscosity would increase by about a factor of ~5 at an applied of pressure of 21 MPa. In contrast, Fig. 9b reveals how much the PDMS viscosity would decrease at any given pressure upon uptake of CO_2 (at that pressure). Thus, incorporation of 30% CO_2 at any given pressure would reduce the polymer melt viscosity by slightly over two orders of magnitude. The opposing trends with pressure and concentration is anticipated as viscosity is influenced by polymer free volume and one expects the free volume to decrease with pressure and increase with CO_2 incorporation [4]. The product of the two shift factors in Fig. 9 would thus give the actual change in viscosity at any given pressure and CO_2 concentration.

Despite the merits of the MLSR, it has its limitations in that the flow is non-viscometric, requiring the use of a constitutive model and calibration with known fluids. However, there are clear advantages that this device provides especially in view of the fact that obtaining any high-pressure measurements in the presence of supercritical fluids is a challenge in itself.

Table 2
Concentration shift factors for viscoelastic scaling of PDMS/CO_2 system at 30 °C

CO_2 concentration (%wt)	a_c
0.000	1.000
0.036	0.336
0.072	0.214
0.088	0.150
0.098	0.196
0.105	0.137
0.128	0.106
0.147	0.086
0.172	0.062
0.182	0.020
0.192	0.034
0.268	0.012
0.298	0.007

First, this device allows measurements of the Newtonian plateau for polymer melts, which is difficult to do with capillary and extrusion rheometers [45]. Secondly, experimental measurements can be taken under conditions of constant pressure at different concentrations of a pressurizing SCF. This enables the effects of pressure and concentration to be decoupled without theoretical modeling. Finally, measurements can be done at high concentrations of CO_2 and/or equilibrium conditions, something that is not possible with other devices. Therefore the use of rheological information gathered from the MLSR and other experimental equipment such as pressurized capillaries or slit dies should provide complementary results that when combined should enable a more complete understanding of the effects of pressurized SCF on a polymer melt. Specifically, the use of multiple devices would allow the effects of temperature, pressure, concentration, and shear rate to be probed over several orders of magnitude, which is not possible with just a single device.

6. Conclusions

In this study, we describe a magnetically levitated sphere rheometer capable of measuring rheological properties of fluids under supercritical conditions, specifically elevated pressures. This magnetically levitated sphere rheometer eliminates many of the disadvantages associated with other high-pressure rheometers. It can operate at a constant pressure, at all concentration regions from pure polymer to an equilibrated polymer/SCF (supercritical fluid) solution, and at varying shear rates. Calibration of the device together with data comparison with traditional rheometers confirms the accuracy of the device and it's ability to produce reliable measurements.

High-pressure experiments on a PDMS/CO_2 system demonstrate the overall utility of the device and it's wide applicability to measuring the rheological properties of polymer/SCF solutions. PDMS/CO_2 mixture viscosity was measured as a function of shear rate at different pressures and concentrations up to 30 wt%. These results revealed that the presence of CO_2 could reduce the viscosity of a PDMS melt by nearly two orders of magnitude. The ability of the MLSR to operate under constant pressure conditions allowed the effects of pressure and CO_2 concentration on the PDMS/CO_2 system to be probed separately. The effects of CO_2 concentrations and pressure have been described by two distinct shift factors, a_c and a_p, which accurately represent the effects of CO_2 and pressure, respectively, on polymer melt rheology.

Acknowledgements

This material is based upon work supported in part by the STC Program of the National Science Foundation under Agreement No. CHE-9876674. The authors also gratefully acknowledge support from the Kenan Center for the Utilization of Carbon Dioxide in Manufacturing at North Carolina State University and the University of North Carolina at Chapel Hill, and the Office of Naval Research award number N00014-98-1-0157. YJG would also like to acknowledge Elf Atochem North America for financial support.

References

[1] McClain J. Chem Engng 2000;107(2):72–9.
[2] Gerhardt LJ, Manke CW, Gulari E. J Polym Sci Part B Polym Phys 1997;35(3):523–34.
[3] Kwag C, Manke CW, Gulari E. J Polym Sci Part B Polym Phys 1999;37:2771–81.
[4] Royer JR, Cray YJ, DeSimone JM, Khan SA J Polym Sci Part B Polym Phys 2000;38:3168.
[5] Lee M, Park CB, Tzoganakis C. Polym Engng Sci 1999;39(1):99–109.
[6] Han CD, Ma C-Y. J Appl Polym Sci 1983;28:851–60.
[7] Han CD, Ma C-Y. J Appl Polym Sci 1983;28:831–50.
[8] Ma C-Y, Han CD. J Cellular Plastics 1982;18:361–70.
[9] Bae YC, Gulari E. J Appl Polym Sci 1997;63:459–66.
[10] Bridgman PW. Proc Am Acad Arts Sci 1926;61:57–99.
[11] Kiran E, Gokmenoglu Z. J Appl Polym Sci 1995;58:2307–24.
[12] Richards WD, Prud'Homme RK. Polym Engng Sci 1987;27(4):294–302.
[13] Koran F, Dealy JM. J Rheol 1999;43(5):1279–90.
[14] Semjonow VV. Rheol Acta 1962;2(2):138–43.
[15] Westover RF. SPE Trans 1961:14–20.
[16] Mackley M, Marshall R, Smeulders J. J Rheol 1995;39(6):1293–309.
[17] Mackley M, Spitteler P. Rheol Acta 1996;35(2):202–9.
[18] Hersey MD, Shore H. Mech Engng 1928;50(3):221–32.
[19] Adam M, et al. Revue Phys Appl 1984;19:253–64.
[20] Chu B, Hilfiker R. Rev Sci Instrum 1989;60(9):3047–50.
[21] Hilfiker R, Chu B, Shook J. Rev Sci Instrum 1989;60(4):760–4.
[22] Gauthier-Manuel B, Meyer R, Pieranski P. J Phys E Sci Instrum 1984;17:1177–82.
[23] Adam M, Delsanti M. Journal De Physique 1983;44(10):1185–93.
[24] Adam M, Aime JP. J Phys II France 1991;1:1277–87.
[25] Adam M, Delsanti M, Durand D. Macromolecules 1985;18:2285–90.
[26] Adam M, Delsanti M. J Physique 1984;45:1513–21.
[27] Adam M, Delsanti M, Okasha R, Hild G J Physique Lett 1979;40:L539–42.
[28] Greer S, Moldover MR, Hocken R. Rev Sci Instrum 1974; 45(11): 1462–3.
[29] Greer S, Hocken R. J Chem Phys 1975;63(12):5067–72.
[30] Millero FJ. Rev Sci Instrum 1967;38(10):1441–4.
[31] Millero FJ, Knox JH, Emmet RT. J Sol Chem 1972;1(2):1972.
[32] Kupke DW, Hodgins MG, Beams JW. Proc Nat Acad Sci 1972;69(8):2258–62.
[33] Ferry JD. Viscoelastic properties of polymers. 3rd ed. New York: John Wiley & Sons, 1980.
[34] Bird RB, Stewart WE, Lightfoot EN. Transport phenomena. New York: John Wiley & Sons, 1960. p. 56–61.
[35] Leal LG. Laminar flow and convective transport processes. Boston: Butterworth-Heinmann, 1992. p. 119–95.
[36] Salem MB, Oesterle B. Int J Multiphase Flow 1998;24(4):563–85.
[37] Davis HA. Rev Sci Instrum 1983;54(10):1412–4.
[38] Roe DC. Organometallics 1987;6(5):942–6.
[39] deLangen M, Prins KO. Rev Sci Instrum 1995;66(11):5218–21.
[40] Horvath IT, Ponce EC. Rev Sci Insturm 1991;62(4):1104–5.
[41] Horvath IT, Millar JM. Chem Rev 1991;91(7):1339–51.
[42] Royer JR, DeSimone JM, Khan SA. Macromolecules 1999;32(26): 8965–73.
[43] Chow TS. Macromolecules 1980;13:362.
[44] Gerhardt LJ, Garg A, Manke CW, Gulari E. J Polym Sci Part B Polym Phys 1998;36:1911–8.
[45] Dealy JM, Wissbrun KF. Melt rheology and its role in plastics processing. New York: Van Nostrand Reinhold, 1989.